Estimating the contribution of Arctic sea-ice loss to central Asia temperature anomalies: the case of winter 2020/2021

ENVIRONMENTAL RESEARCH
LETTERS

PURPOSE-LED PUBLISHING™

LETTER • OPEN ACCESS

Estimating the contribution of Arctic sea-ice loss to central Asia temperature anomalies: the case of winter 2020/2021

To cite this article: Lara R Cosford *et al* 2025 *Environ. Res. Lett.* **20** 034007

ENVIRONMENTAL RESEARCH
LETTERS

LETTER

Estimating the contribution of Arctic sea-ice loss to central Asia temperature anomalies: the case of winter 2020/2021

Lara R Cosford[1], **Rohit Ghosh**[1,2], **Marlene Kretschmer**[1,3], **Clare Oatley**[4] and **Theodore G Shepherd**[1,*]

[1] Department of Meteorology, University of Reading, Reading, United Kingdom
[2] Alfred Wegener Institute, Helmholtz Centre for Polar and Marine Research, Bremerhaven, Germany
[3] Institute for Meteorology, Leipzig University, Leipzig, Germany
[4] RWE Supply and Trading Gmbh, London, United Kingdom
[*] Author to whom any correspondence should be addressed.

E-mail: theodore.shepherd@reading.ac.uk

Keywords: stratosphere, Arctic sea ice, central Asia temperature

OPEN ACCESS

RECEIVED
12 September 2024

REVISED
13 December 2024

ACCEPTED FOR PUBLICATION
24 January 2025

PUBLISHED
11 February 2025

Abstract

Arctic sea-ice cover has declined drastically in recent decades, notably in the Barents-Kara Seas (BKS). Previous research has linked low autumn BKS-ice cover to subsequent cold Eurasian winters. This lagged relationship was observed in 2020/2021. Using a causal network framework grounded in known physical mechanisms, we assess how strongly one factor directly influences another (i.e. the causal relationship) and apply this analysis to the anomalies from 2020/2021. We show that although year-to-year BKS-ice variations have only a minor impact on Central Asia temperatures, that causal effect becomes important for attribution and prediction when we consider the large long-term trend in BKS-ice cover. In particular, we find that Central Asia's 2021 negative winter surface air temperature anomaly (relative to 1980–2020) can be fully explained by the BKS-ice anomaly. We further estimate that BKS-ice loss has more than halved the winter warming over Central Asia over the past 40 years. Hence rather than debating a cooling trend in Central Asia during winter, we propose shifting the focus to the influence of Arctic Amplification on anticipated warming trends. This study illustrates the efficacy of causal network analysis, which has implications for seasonal prediction and attribution of midlatitude winter anomalies.

1. Introduction

Previous studies have identified a potential relationship between anomalously low autumn sea-ice extent in the Barents and Kara Seas (BKS), and extremely cold surface (2m) air temperature (SAT) anomalies across Eurasia during the following winter. The proposed lagged relationship is thought to occur by both a tropospheric and a stratospheric pathway (Kretschmer *et al* 2016, 2018, Outten *et al* 2023). Although the exact mechanisms and effect strengths are still debated, it is assumed that warming of the Arctic lower troposphere due to low BKS sea-ice extent forces a stationary Rossby wave (Honda *et al* 2009, Kim *et al* 2014) which strengthens the Siberian High and intensifies Ural blocking (UB) (Honda *et al* 2009, Gong and Luo 2017, Mori *et al* 2019, Peings 2019, Tyrlis *et al* 2019, Ghosh *et al* 2024, Kaufman *et al* 2024), and encourages a negative phase of the Arctic Oscillation (AO) and North Atlantic Oscillation (NAO) (Deser *et al* 2004, Jeong and Ho 2005, Nakamura *et al* 2016a, 2016b, Siew *et al* 2020), all of which favours cold Eurasian SATs. The stratospheric pathway, in contrast, refers to weakening of the stratospheric polar vortex (SPV) in response to BKS sea-ice loss and the associated intensified UB, which interferes constructively with the climatological waves, thereby promoting enhanced upward-propagating planetary waves (Kim *et al* 2014, Kretschmer *et al* 2018). The stratospheric anomalies then propagate downwards into the troposphere (Baldwin and Dunkerton 2001) and affect winter tropospheric circulation, for example by inducing a negative AO phase (Kim *et al* 2014, Nakamura *et al* 2015, King *et al* 2016, Zhang *et al* 2018).

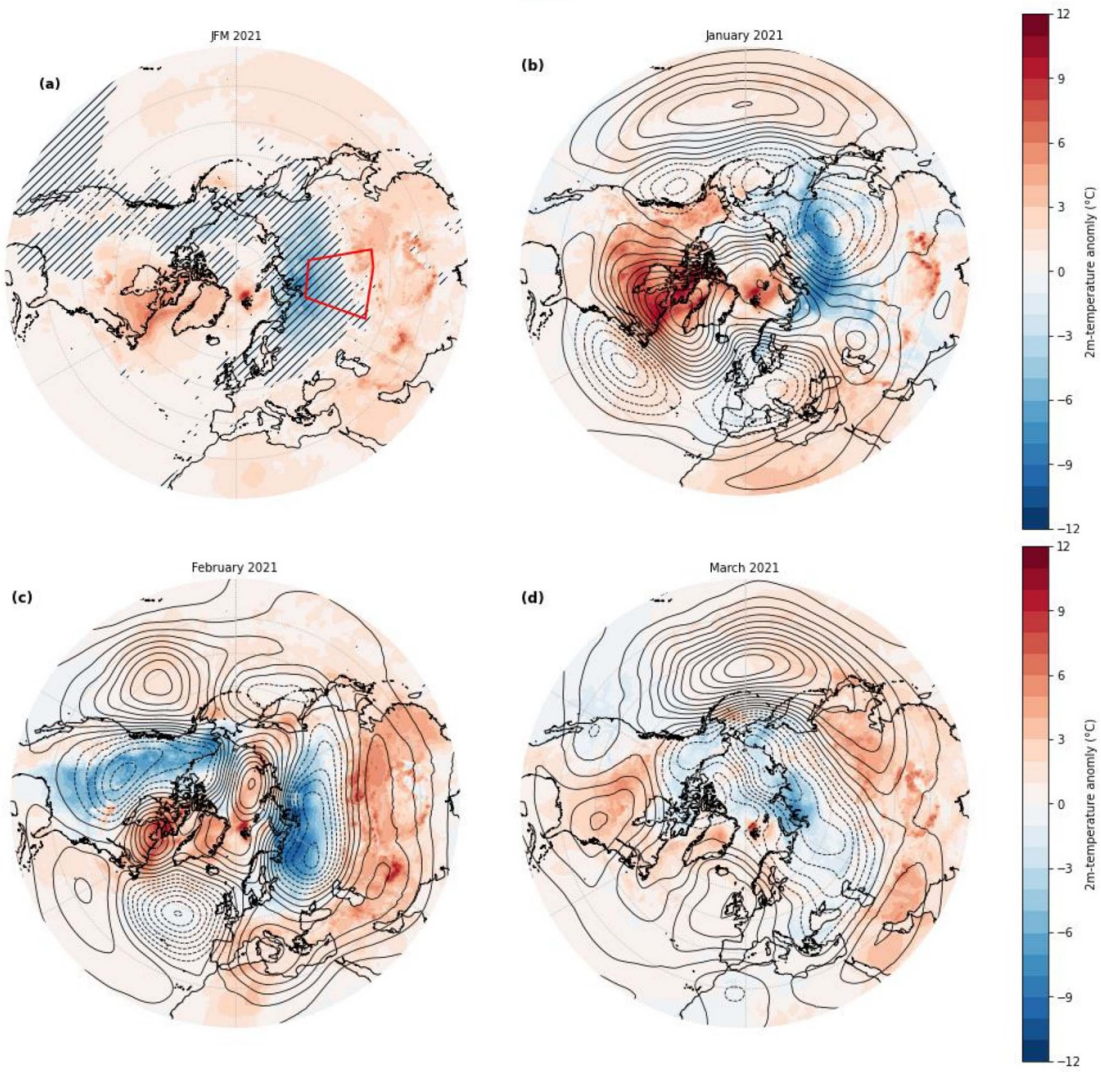

Figure 1. (a) JFM average 2021 2m temperature anomalies (shading) with average 500 hPa geopotential height (Z500) anomaly contours (20 m interval), plotted over the Northern Hemisphere (20°N-90°N). (b), (c), (d) As in (a), but for January 2021, February 2021 and March 2021 respectively. All figures are produced using ERA5 reanalysis data (Hersbach *et al* 2020). The climatological reference period is 1979/1980–2019/2020. In panel (a) only, hatching shows values at least one standard deviation below the mean. The red box shows the region over which the CAT index is computed.

However, it can be difficult to isolate these specific pathways and determine which has principal influence. This has led to widely varying results across observational and modelling studies regarding the winter mid-latitude circulation and temperature response to Arctic sea-ice decline (McCusker *et al* 2016, Blackport *et al* 2019, Blackport and Screen 2020, 2021, Peings *et al* 2021, Zappa *et al* 2021, Komatsu *et al* 2022, Sun *et al* 2022, Wang and Chen 2022, Outten *et al* 2023). As a result, the Arctic-midlatitude relationship is still under debate, and in particular, it remains unclear whether this relationship is strong enough to be useful in seasonal prediction and attribution (Barnes and Screen 2015).

Winter 2020/2021 provides an example of this hypothesised lagged relationship between low BKS and cold Eurasian SAT. Monthly near-surface temperature anomalies were as much as 10 °C below the reference climate period (winter 1979/1980 through winter 2019/2020, referred to subsequently as the 1980–2020 period) across Eurasia (figure 1). This followed an autumn in which there was anomalously low sea-ice extent and anomalously high SAT observed in the BKS. Other important atmospheric features include a sudden stratospheric warming (SSW) that occurred in January 2021, that is, a rapid weakening of the SPV, followed by a negative phase of the AO. Thus, this winter presents what would appear to be a textbook example of the hypothesised BKS midlatitude SAT relationship, and has already been the subject of research. For example, Nishii *et al* (2022) argued using ensemble experiments of an atmospheric general circulation model that Arctic sea-ice decline contributed to Eurasian cooling in

December 2020, but that neither sea-ice decline nor sea surface temperature anomalies can explain the negative Eurasian SATs or the negative AO observed in January 2021.

Although model experiments can establish causality, model biases preclude applying the inferences directly to the real climate system. AMIP-type experiments, for example, are limited in their ability to create a realistic simulation of atmosphere–ocean-sea-ice coupled interactions, creating an over-simplistic and potentially misleading understanding of the complex and dynamic response of the atmosphere to sea-ice loss (Deser *et al* 2015, 2016, Graff *et al* 2019, Blackport and Screen 2021, Liang *et al* 2021). Instead, we follow a complementary approach using causal networks and observational data. The rationale behind such an approach is not to prove the causality of the relationships—for that, we rely on previous literature—but, rather, to quantify the hypothesised causal relationships in the presence of confounding factors and estimate their contribution to the 2020/2021 winter anomalies. We first use observational data to compare the meteorological conditions during the autumn and winter of 2020/2021. We then use causal network analysis on a seasonal timescale as outlined by Kretschmer *et al* (2021) (hereafter referred to as K21), and discussed further below, to quantify the average causal effect of BKS on Eurasian SATs via the stratospheric and tropospheric pathways using data from the 1980–2020 reference period. Based on this analysis, we quantify the contribution of BKS to the cold Eurasian winter in 2020/2021, and discuss different ways how this can be interpreted, which might partly explain the competing claims from different researchers concerning Arctic-midlatitude connections.

2. Data and methods

We utilised ERA5 reanalysis data in the extended winter (October to March) from 1979/1980–2020/2021 (Hersbach *et al* 2020), here referred to as observations. To attribute and predict temperatures in Central Asia using BKS ice loss, we apply a causal network approach as explained in detail in K21. Causal networks are used to represent hypothesised physical relationships in the climate system, which facilitates their statistical analysis. In particular, it allows for better understanding of how causal information flows and easier identification of confounding variables. We adapt K21's example 4 to explore the linear relationship between autumn BKS and Eurasian winter SATs and create multiple linear regression equations that reflect the specific teleconnections involved in the occurrence of cold Eurasian temperatures. Our aim in MLR analysis is to quantify the lagged causal relationship between autumn 2020 (OND) BKS and winter 2021 (JFM) Central Asia 2 metre temperature (CAT) (keeping the seasons consistent with Kretschmer *et al* 2020) via both the stratospheric and tropospheric pathways. We choose not to investigate the lagged relationship between individual months due to the large amount of noise in the system, and the expected non-stationarity of the causal relationship within the season. Given the small sample size of the observational record we also choose not to investigate potential nonlinearities in the causal relationship, or the role of sea-ice changes in other regions of the Arctic. Any such influences will appear in our residuals as unexplained variance. Importantly, the analysis framework does not address the cause of the BKS anomaly, thus does not differentiate between internal variability and forced effects. It merely quantifies the effect of that anomaly (however it is caused) on the SPV and on CAT. The logic behind the analysis is discussed further below.

For this causal network-guided MLR analysis, we create time-series indices of the involved processes by area-averaging over different regions and variables. Indices include UB (sea level pressure over 40°E–85°E and 45°N–70°N), North Pacific blocking (NP; sea level pressure over 35°N–65°N and 160°E–140°W), the SPV (10 hPa zonal mean zonal wind over 55°N–65°N), BKS ice (sea ice fraction over 65°N–85°N and 20°E–90°E) and CAT (2 m temperature over 45°N–65°N and 70°E–100°E). The geographic areas for each index follow K21.

The anomalies of these timeseries are created by subtracting the mean value over the 41 year reference period (without winter 2020/2021). Before the indices were used to train the MLR models, they were linearly detrended and then standardised. The resulting MLR coefficients are then used to predict the relevant indices for winter 2020/2021.

3. Results

The autumn/winter of 2020/2021 was characterised by low sea ice and high SAT. October displayed the most extreme sea-ice fraction (SIF) anomalies, reaching as low as −90%, followed by negative anomalies in November and December, albeit less severe (figure 2). Z500 anomalies showed a distinct wave-like pattern in January and February (figures 1(b) and (c)), with strong negative anomalies over western Europe, northeast Asia, and the North Pacific, alongside strong positive anomalies over the BKS, Greenland, and northeast Canada. The pattern mirrored that observed in Kim *et al* (2014), suggesting a recurring climatic pattern. A notable event occurred on 5 January 2021 with the occurrence of an SSW (L'heureux 2021), leading to a rapid weakening of the SPV. Anomalously high geopotential heights appeared in the upper stratosphere at the start of January, propagating downward through the stratosphere over the course of

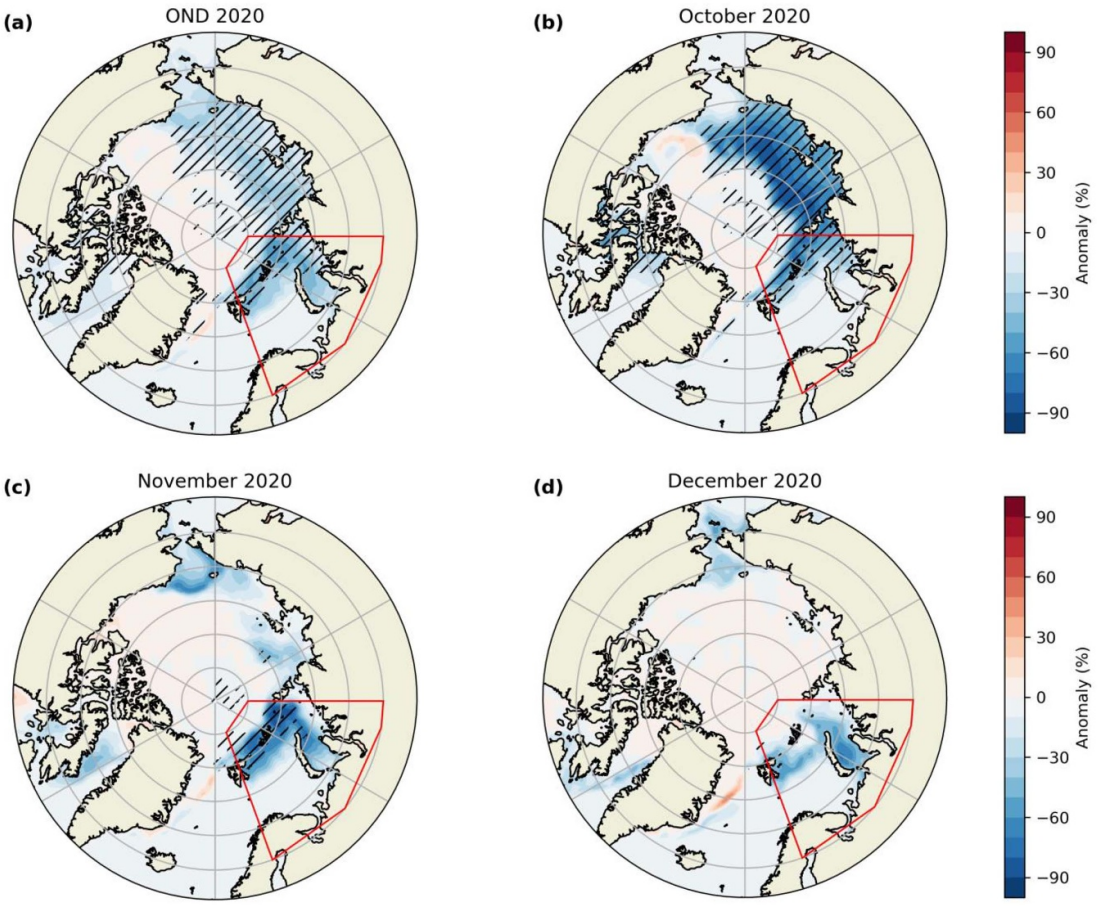

Figure 2. Arctic sea-ice fraction anomalies (%) from their respective long-term means (1980–2020) observed across the northern polar circle (60°N–90°N) in (a) OND 2020 (seasonal average), (b) October 2020, (c) November 2020 and (d) December 2020. The climatological reference period is 1979/1980–2019/2020. Hatching shows values at least one standard deviation below the mean. The red box shows the region over which the BKS index is computed.

the month and eventually reaching the troposphere by late January/early February (figure 3). Conversely, anomalously low geopotential heights were observed in the upper stratosphere in mid-February, gradually propagating downward through the stratosphere and reaching the troposphere by the end of March, though decreasing in strength at the longer lead times. These observations support the hypothesised dynamic coupling between the stratosphere and troposphere, as suggested by numerous previous studies (e.g. Baldwin and Dunkerton 2001, Kim *et al* 2014, Baldwin *et al* 2020, Vargin *et al* 2022).

Following the January SSW event, a strong negative AO and NAO persisted for the remainder of the month. This atmospheric pattern was associated with a persistent trough, bringing colder than average temperatures over Europe and northern Asia. In January, temperatures were approximately 2 °C colder than average over northern Asia (NOAA 2021a) (as seen in figure 1(b)), while in February, the strong negative AO persisted, resulting in temperatures at least 3 °C below the 20th-century baseline (NOAA 2021b) (as seen in figure 1(c)). These temperature anomalies underscore the significant impact of atmospheric circulation patterns on regional climate conditions, highlighting the interconnectedness of atmospheric dynamics and surface climate variability.

Before quantifying the contributions of BKS for winter 2020/2021, we examine the time series of the relevant indices (figure 4). Both the original trended time series (solid) and detrended time series (dashed) are presented. A clear long-term decline is apparent in the BKS index, while the trends in the other indices are small compared to the variability. While the BKS anomaly in autumn 2020 (corresponding to winter 2021 in figure 4(a)) is one of the very lowest in the post-1980 record, the corresponding detrended anomaly value is not. The 2021 winter SPV anomaly is negative but not particularly extreme (figure 4(d)), but the UB anomaly is exceptionally positive (figure 4(b)). As for CAT, the 2021 winter anomaly is negative both for the trended and detrended data (figure 4(e)).

We now demonstrate, using winter 2020/2021 as a case study, how causal network analysis may be used for seasonal prediction of Eurasian winter temperatures. We further attempt to assign a percentage

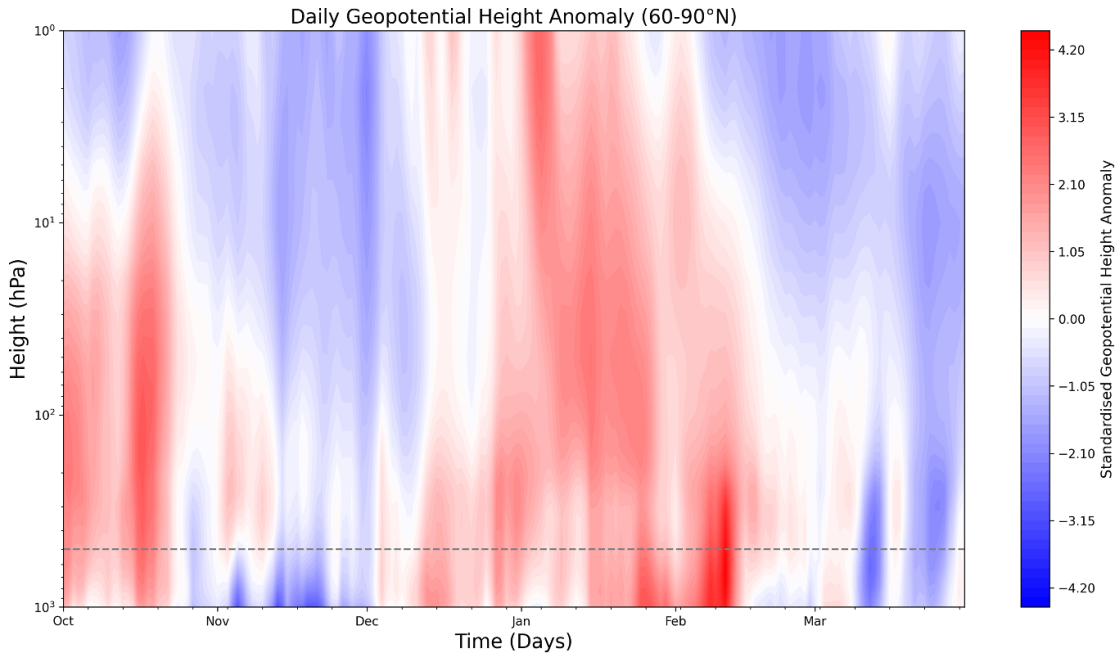

Figure 3. Area-averaged Arctic (60–90°N) 2020/2021 daily geopotential height anomaly (in standardised units), relative to the climatological reference period of 1979/1980–2019/2020. The dashed grey line represents the approximate location of the tropopause.

influence that BKS in autumn 2020 has on CAT in winter 2021, via both the stratospheric and tropospheric pathways, hence perform an attribution of the event. Finally, we place this winter in the context of the longer-term trend.

Based on previous literature in the field of Arctic mid-latitude connections, figure 5 displays the assumed causal pathways by which autumn BKS is understood to causally influence wintertime Eurasian temperatures. The figure includes both the reported stratospheric pathway (via the SPV, blue arrows) and the direct tropospheric pathway (red arrow). Moreover, it highlights the complex influence of autumn UB, which acts as a confounder as it influences autumn BKS as well as the winter SPV and winter CAT (Kretschmer *et al* 2016, 2020, Luo *et al* 2016a, 2016b, Tyrlis *et al* 2019). Note that a mediating role of winter UB from BKS to CAT is considered but assumed to only be relevant after the autumn months (OND), and therefore not explicitly shown in the network. Thus, importantly, we explicitly allow for the possibility that autumn UB may be a driver of BKS. We further include the confounder autumn NP, potentially influencing both autumn BKS as well as winter SPV. By controlling for the influence of autumn UB and NP, we can isolate the causal effect of BKS on CAT, irrespective of the cause of BKS (see details below). Note that more remote influences on BKS, such as ENSO or autumn snow cover, are captured by this network since they are understood to be mediated by either autumn UB or autumn NP (see also K21).

To quantify the effect of BKS on CAT via the tropospheric pathway (red arrow in figure 5), we refer to example 3 outlined by K21. In this 'direct' tropospheric pathway, BKS affects CAT, for example via enhanced UB in winter. To isolate this pathway in the data, it is necessary to regress out the effect of the stratospheric pathway, which involves the contemporaneous effect of the SPV on CAT, as well as the confounding tropospheric effect of autumn UB. We therefore condition on SPV during JFM and UB in OND and the appropriate MLR equation becomes:

$$\mathrm{CAT}_{\mathrm{JFM}} = \alpha_1 \mathrm{BKS}_{\mathrm{OND}} + \beta_1 \mathrm{SPV}_{\mathrm{JFM}} + \gamma_1 \mathrm{UB}_{\mathrm{OND}} + \varepsilon. \quad (1)$$

The results of this causal pathway are displayed in table 1. The α_1 coefficient is 0.23 ± 0.16, meaning that a 1 standard-deviation detrended anomaly in BKS leads to a 0.23 standard-deviation detrended anomaly in CAT through the tropospheric pathway. In other words, the year-to-year variability in BKS explains less than 10% of the variance $(0.23)^2 = 0.05$ in the year-to-year CAT variability through the tropospheric pathway. Estimated this way, its contribution in 2020/2021 would be small since the detrended BKS anomaly was not particularly large (-1.07). However, multiplying α_1 by the autumn 2020 BKS trended anomaly (-3.07), a value of -0.70 ± 0.49 is obtained. This exceeds the winter 2021 CAT trended anomaly (-0.64), relative to the 1980–2020 reference period (figure 6). Before reflecting on this perhaps surprising result, we complete the MLR analysis.

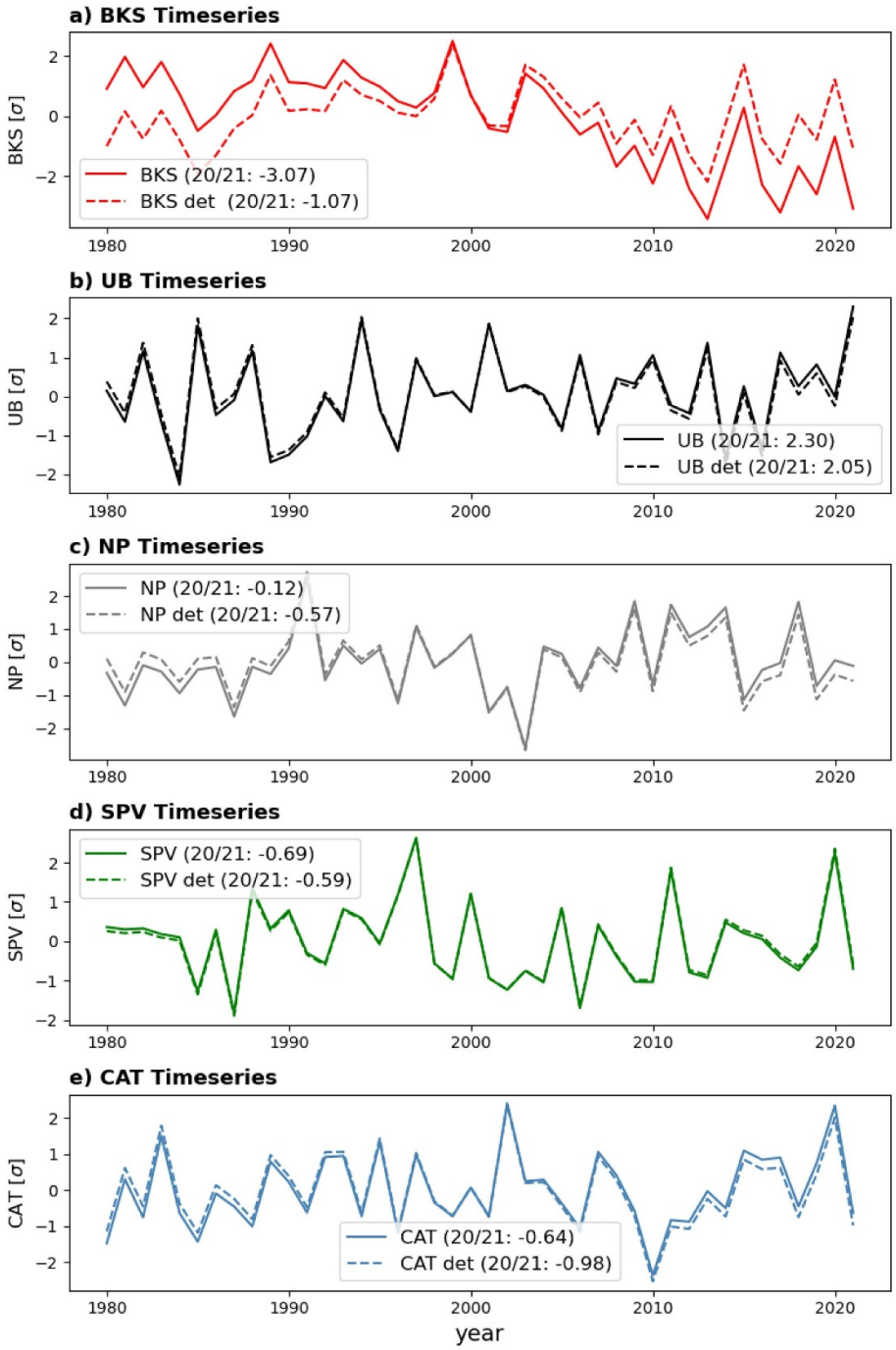

Figure 4. The trended (solid) and detrended (dashed) time series for (a) BKS index (OND), (b) UB index (OND), (c) NP index (OND), (d) SPV index (JFM) and (e) CAT index (JFM), for the period 1980–2021, presented in standardised units of one standard deviation of the detrended time series (excluding autumn/winter 2020/21). The values in 2020/21 are provided in the inset. Although the BKS, UB and NP indices are created using data from OND 1979–2020, for simplicity the *x* axis on each plot refers to the winter years, i.e. 1980–2021.

The stratospheric pathway (blue arrows in figure 5) can be split into two parts. The first part is the teleconnection from BKS to SPV, which is proposed to be mediated via winter UB (Kim *et al* 2014, Kretschmer *et al* 2016). However, UB also influences BKS (Tyrlis *et al* 2019), hence acts as a common driver of SPV and BKS (grey arrows in figure 5), making it necessary to regress out its influence. Additionally, NP can also influence both BKS and SPV (grey arrows in figure 5), and therefore needs to be regressed out. We follow the methodology in K21 and condition on UB and NP in the same months as BKS (OND), assuming that the mediating role of UB involves a time-lag and is therefore not regressed out this way. The MLR equation to express the effect of BKS on SPV is therefore (K21):

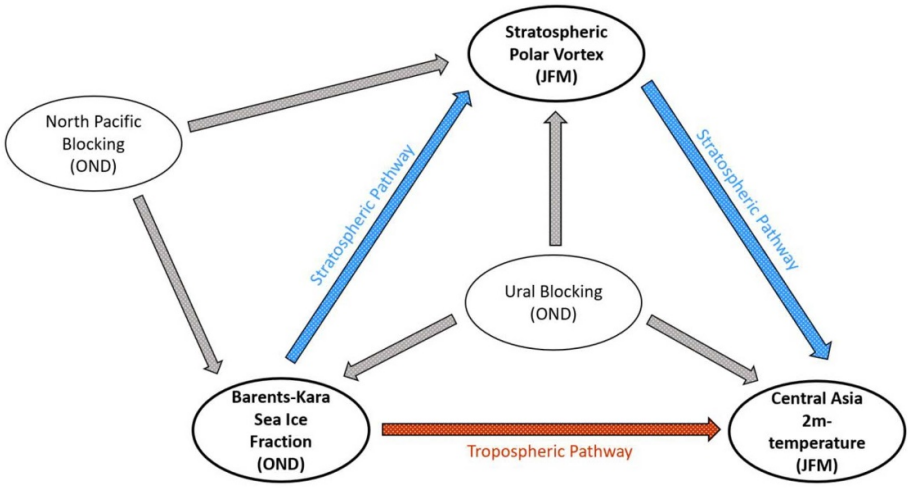

Figure 5. The hypothesised causal pathways between autumn (OND) Barents-Kara sea-ice fraction (BKS) and winter (JFM) Central Asia 2 metre temperature (CAT). The tropospheric pathway is shown in red and the stratospheric pathway via the winter stratospheric polar vortex (SPV) in blue. Ural blocking (UB) and North Pacific blocking (NP) in autumn are also included due to their confounding effects on BKS, SPV and CAT.

$$\mathrm{SPV_{JFM}} = \alpha_2 \mathrm{BKS_{OND}} + \beta_2 \mathrm{NP_{OND}} + \gamma_2 \mathrm{UB_{OND}} + \varepsilon \quad (2)$$

where the regression coefficient α_2 (0.22 ± 0.15) is the effect from BKS to SPV we aim to isolate (table 1). The values of the regression coefficients from K21 are provided for comparison, and are found to be entirely consistent with our values.

These coefficients are however for the year-to-year variability as reflected in the detrended timeseries. If we consider the actual (trended) values, then as with the tropospheric pathway, a different picture emerges. Multiplying the regression coefficient α_2 from equation (2) (0.22 ± 0.15) by the autumn 2020 BKS standardised trended value (-3.07), a value of -0.68 ± 0.46 is obtained. This can fully account for the trended value of the winter 2021 SPV anomaly (-0.69). Thus, although the year-to-year variability of BKS explains only a small amount of the year-to-year SPV variability, the long-term decline in BKS can be a very significant causal factor for SPV anomalies relative to a historical baseline.

The second part of the stratospheric pathway is the influence of SPV on CAT. To isolate this effect, we take the regression coefficient β_1 from equation (1) (0.15 ± 0.16), which represents the effect from SPV on CAT after controlling for the common drivers BKS and UB. By multiplying together both components of the stratospheric pathway, that is, the causal effect of BKS on SPV (0.22 ± 0.15) and of SPV on CAT (0.15 ± 0.16), we get the total effect of BKS on CAT via the stratospheric pathway as 0.033 ± 0.042. This is much smaller than the value of 0.23 ± 0.16 found for the tropospheric pathway. Note that this stratospheric-pathway effect is, like the tropospheric-pathway effect, already predictable from autumn conditions. If the winter SPV value is already known, then its causal effect on winter CAT (0.15 ± 0.16) is more comparable to that of BKS (0.23 ± 0.16), however that is of no use for seasonal prediction since that effect is synchronous.

The total effect of autumn BKS on winter CAT can finally be quantified by calculating the sum of the effects each of these pathways has on CAT, i.e.:

$$\begin{aligned}\mathrm{Total}\ (\alpha_3) &= \mathrm{Tropospheric} + \mathrm{Stratospheric} \\ &= \alpha_1 + (\alpha_2 \times \beta_1)\end{aligned} \quad (3)$$

which adds up to $(0.23 \pm 0.16) + (0.033 \pm 0.042) = 0.26 \pm 0.17$ and represents the total standardised effect of BKS on CAT via both pathways (table 1).

Note that the sum of the tropospheric and stratospheric pathways (described above) is equivalent to the estimate of the total contribution from BKS to CAT using MLR based on figure 5

$$\mathrm{CAT_{JFM}} = \alpha_4 \mathrm{BKS_{OND}} + \beta_4 \mathrm{NP_{OND}} + \gamma_4 \mathrm{UB_{OND}} + \varepsilon. \quad (4)$$

The α_4 coefficient from this equation is equal to 0.25 ± 0.16, which is similar (within uncertainties) to the estimate of 0.26 ± 0.17 from summing the tropospheric and stratospheric pathways (table 1).

We now discuss the overall attribution results as represented in figure 6. Multiplying the 2021 BKS detrended anomaly (-1.07) by the total effect of both the tropospheric and stratospheric pathways (0.26 ± 0.17) gives a value of -0.28, which only represents 29% of the 2021 CAT detrended anomaly of -0.98. Thus, the influence of BKS on CAT appears

Table 1. Results of the regression coefficients from equations (1)–(4) and associated standard errors. Calculations of the influence of BKS on winter CAT (α_1 in equation (1)), BKS on the winter SPV (α_2 in equation (2)), and SPV on CAT (β_1 in equation (1)) are also provided.

	Coefficient	Standard error	K21
Equation (1)			
α_1	0.23	0.16	—
β_1	0.15	0.16	—
γ_1	−0.14	0.16	
Influence of BKS on CAT via the tropospheric pathway Detrended: $(0.23 \pm 0.16) \times (-1.07) = -0.25 \pm 0.17\,(25 \pm 17\%)$ Trended: $(0.23 \pm 0.16) \times (-3.07) = -0.70 \pm 0.49\,(109 \pm 77\%)$			
Equation (2)			
α_2	0.22	0.15	0.21
β_2	0.24	0.15	0.27
γ_2	−0.16	0.16	0.00
Influence of BKS on SPV Detrended: $(0.22 \pm 0.15) \times (-1.07) = -0.24 \pm 0.16\,(41 \pm 27\%)$ Trended: $(0.22 \pm 0.15) \times (-3.07) = -0.68 \pm 0.46\,(99 \pm 67\%)$			
Influence of BKS on CAT via the stratospheric pathway Detrended: $(0.22 \pm 0.15) \times (0.15 \pm 0.16) \times (-1.07) = -0.035 \pm 0.045\,(4 \pm 5\%)$ Trended: $(0.22 \pm 0.15) \times (0.15 \pm 0.16) \times (-3.07) = -0.10 \pm 0.13\,(16 \pm 20\%)$			
Equation (3)			
α_3	0.26	0.17	—
Total effect of BKS on CAT via both pathways Detrended: $(0.26 \pm 0.17) \times (-1.07) = -0.28 \pm 0.18\,(29 \pm 18\%)$ Trended: $(0.26 \pm 0.17) \times (-3.07) = -0.80 \pm 0.52\,(125 \pm 81\%)$			
Equation (4)			
α_4	0.25	0.16	—
β_4	−0.13	0.15	—
γ_4	−0.20	0.16	—

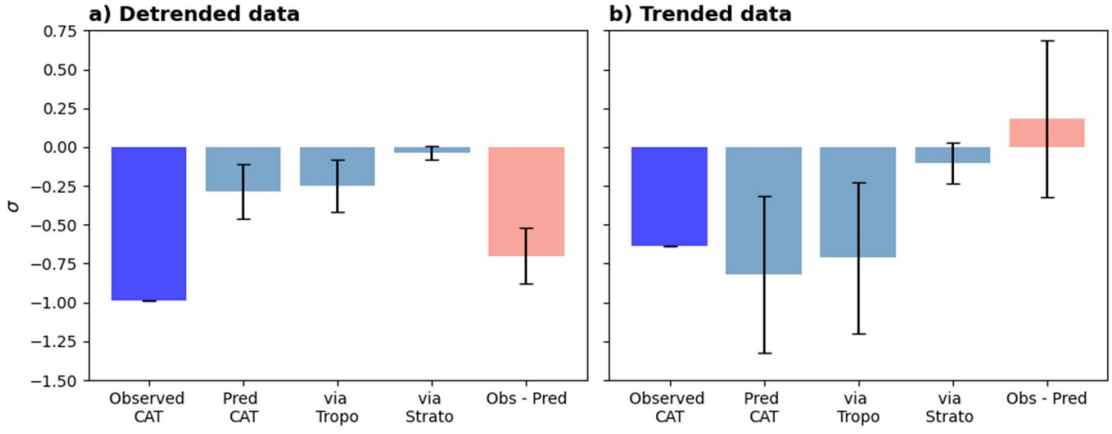

Figure 6. Observed and estimated Central Asia temperature (CAT) anomaly in winter 2020/21 for (a) the detrended data and (b) the trended data. Shown are the observed values (blue bars) in that winter, and the prediction based on the total effect of BKS and on the separate estimates of the tropospheric and stratospheric pathways. The red bars show the difference between the observed and predicted values. All values are shown in units of standard deviations of the detrended timeseries over the reference period (see methods). The whiskers in the middle bars indicate the standard errors.

to be modest in terms of explaining the year-to-year variability.

However, the influence of BKS on yearly anomalies relative to a long reference period over which BKS has substantially declined is considerably larger. Indeed, the total causal effect of the 2021 BKS trended anomaly is more than sufficient ($125 \pm 81\%$) to explain the 2021 CAT trended anomaly. What that means is that in a counterfactual world without BKS decline, we could have expected the 2021 CAT anomaly, relative to 1980–2020, to have been positive rather than negative. That is not a particularly radical proposition, given that we are living in a warming world.

We can also calculate the contribution of the BKS decline to the CAT trend. Multiplying the total decline in the BKS index over the reference period (-4.00 in standardised units) by the effect of both pathways (0.26 ± 0.17) gives the total effect of the BKS trend on the CAT trend over 42 years. This value is -1.04 ± 0.68, which equates to -2.11 ± 1.38 °C in physical units, given that the standard deviation of the detrended CAT timeseries is 2.03 °C. Since the observed warming of CAT over 42 years was 1.36 °C, we thus infer that without the BKS decline the warming over the same period would have been 3.47 °C. In other words, the warming trend in winter CAT between 1979 and 2021 has been more than halved by BKS reduction. Of course, there are large uncertainties on these numbers.

From figure 4(d) we saw that there is essentially no long-term trend in winter SPV. Yet, based on our estimates, the long-term BKS decline can be expected to have induced a long-term decline in SPV of $-4.00 \times (0.22 \pm 0.15) = -0.88 \pm 0.60$ in standardised units, which equates to -7.2 ± -4.9 m s^{-1} in physical units. Such a decline would be difficult to detect statistically, but suggests that without BKS decline the SPV would have strengthened rather than exhibiting basically no trend. This is consistent with climate models showing a strengthening of the SPV under climate change after the sea ice-induced weakening is removed (Kretschmer *et al* 2020). Thus, our results are consistent with the hypothesis that the expected strengthening of the SPV under climate change has been approximately offset over the years by BKS decline.

We finally comment on the role of UB trends in our analysis, since they have been a topic of some discussion (e.g. Kaufman *et al* 2024). Over the reference period analysed here, the OND UB index has increased by 0.5 in standardised units. The correlation between detrended OND UB and BKS is -0.26. Assuming this represents a direct causal link from OND UB to BKS, this implies that the long-term trend in OND UB has provided -0.13 of the long-term BKS decline of -4.00 over this period, which is negligible. Yet the extreme high OND UB in 2020/21 of 2.30 contributed -0.64 to the low BKS that year, so was not a negligible factor in that particular year. Further, the causal effect from OND UB to CAT of -0.14 from equation (1) suggests that the trend in UB has contributed -0.07 towards the long-term trend in CAT, which is negligible compared to the estimated BKS contribution of -1.04.

4. Discussion and conclusions

We investigated the role of BKS-ice decline in the extreme CATs observed in 2020/2021 winter, using ERA5 reanalysis data to construct atmospheric teleconnection indices that are hypothesised to act as common or mediating drivers in the relationship. To do this, we applied MLR analysis to quantify the relative contributions from the tropospheric and stratospheric pathways based on a causal network approach (figure 5). It appears that the effect of BKS on CAT is strongly dominated by the tropospheric pathway. This is an important source for seasonal predictability, because its effect can be computed already in autumn, and does not rely too much on stratospheric variability. Seasonal prediction models should be further evaluated to understand biases in capturing these linkages.

The large standard errors related to the regression coefficients suggest a high degree of uncertainty when attempting to quantify the effect of BKS on CAT. Thus, this approach should not be considered as a replacement to predictions by seasonal forecast models, or model-based attribution, but instead showcases an alternative approach which may be used to complement other analyses. In particular, causal networks serve as a means to develop quantitative hypotheses and plausible storylines. As emphasised in K21, they facilitate straightforward statistical analysis of data and offer a framework for articulating and quantifying both direct and indirect teleconnection pathways (Outten *et al* 2023).

With these caveats in mind, our results suggest that in terms of the year-to-year variability, BKS has a minimal effect on CAT, and this was also the case in 2020/2021. This is consistent with Nishii *et al* (2022) (section 1), who also find a limited relationship with January temperatures in particular, when using climate model experiments. However, when we consider the long-term decline in BKS, we get an entirely different picture (figure 6). In particular, our analysis implies that without the long-term BKS decline, the CAT anomaly (relative to 1980–2020) would have been positive rather than negative. Overall, the results highlight the importance of BKS as a source, and causal networks as a statistical framework for seasonal predictability and attribution, when the historical reference period includes a strong trend in one of the explanatory variables. That trend is already loading

the dice, and needs to be reflected in the attribution statements.

Additionally, when analysing the long-term trend in the CAT time series, our results suggest that BKS decline has roughly halved the expected warming from greenhouse gas increases. Given that there is evidently a tug-of-war between a BKS-induced wintertime cooling trend in Central Asia and an overall global warming trend from climate change in the absence of BKS changes, a focus on the sign of the net temperature trend is not the most physically informative approach. Indeed, this may be one of the reasons for the apparently contradictory findings reported in the literature. For example, if the observed CAT anomaly in 2021 was only slightly warmer, then it could have been positive rather than negative, and it would not have made sense to have described the BKS-induced CAT cooling as a percentage of the observed anomaly. This shows the limitations of fractional attribution statements when different causal factors are operating in opposite directions, and the importance of bringing physical reasoning into the statistical analysis (Shepherd 2021). Instead of debating a wintertime cooling trend in Central Asia (see e.g. Blackport *et al* 2024), we suggest that focus should shift to how Arctic Amplification impacts expected warming trends.

Data availability statement

The data that support the findings of this study are openly available at the following URL/DOI: https://cds.climate.copernicus.eu/#!/home.

Acknowledgment

MK and TGS acknowledge funding from the UK NERC Project ArctiCONNECT and the project XAIDA, funded through the European Union's Horizon 2020 research and innovation programme under Grant Agreement No. 101003469. MK further acknowledges funding by the Deutsche Forschungsgemeinschaft (DFG, German Research Foundation) – Project Number 268020496 – TR 172, within the framework of the Transregional Collaborative Research Centre 'ArctiC Amplification: Climate Relevant Atmospheric and SurfaCe Processes, and Feedback Mechanisms (AC)^3'. We thank the editor and two reviewers for their constructive feedback which has helped to improve the paper.

Open data and code

Code used to create this statistical analysis can be found at the following link https://github.com/marlenek13/2024_Cosford_etal.

ORCID iDs

Lara R Cosford https://orcid.org/0009-0009-0504-8939
Rohit Ghosh https://orcid.org/0000-0001-9888-7292
Marlene Kretschmer https://orcid.org/0000-0002-2756-9526
Theodore G Shepherd https://orcid.org/0000-0002-6631-9968

References

Baldwin M P *et al* 2020 Sudden stratospheric warmings *Rev. Geophys.* **59** e2020RG000708
Baldwin M P and Dunkerton T J 2001 Stratospheric harbingers of anomalous weather regimes *Science* **294** 581–4
Barnes E A and Screen J A 2015 The impact of Arctic warming on midlatitude jet-stream: can it? Has it? Will it? *WIREs Clim. Change* **6** 277–86
Blackport R and Screen J A 2020 Weakened evidence for mid-latitude impacts of Arctic warming *Nat. Clim. Change* **10** 1065–6
Blackport R and Screen J A 2021 Observed statistical connections overestimate the causal effects of Arctic sea ice changes on midlatitude winter climate *J. Clim.* **34** 3021–38
Blackport R, Screen J A, van der Wiel K and Bintanja R 2019 Minimal influence of reduced Arctic sea ice on coincident cold winters in mid-latitudes *Nat. Clim. Change* **9** 697–704
Blackport R, Sigmond M and Screen J A 2024 Models and observations agree on fewer and milder midlatitude cold extremes even over recent decades of rapid Arctic warming *Sci. Adv.* **10** eadp1346
Deser C, Magnusdottir G, Saravanan R and Phillips A 2004 The effects of North Atlantic SST and sea ice anomalies on the winter circulation in CCM3. Part II: direct and indirect components of the response *J. Clim.* **17** 877–89
Deser C, Terray L and Phillips A S 2016 Forced and internal components of winter air temperature trends over North America during the past 50 years: mechanisms and implications *J. Clim.* **29** 2237–58
Deser C, Tomas R A and Sun L 2015 The role of ocean–atmosphere coupling in the zonal-mean atmospheric response to Arctic sea ice loss *J. Clim.* **28** 2168–86
Ghosh R *et al* 2024 Observed winter Barents Kara Sea ice variations induce prominent sub-decadal variability and a multi-decadal trend in the warm Arctic cold Eurasia pattern *Environ. Res. Lett.* **19** 024018
Gong T and Luo D 2017 Ural blocking as an amplifier of the Arctic sea ice decline in winter *J. Clim.* **30** 2639–54
Graff L S, Iversen T, Bethke I, Debernard J B, Seland Ø, Bentsen M, Kirkevåg A, Li C and Olivié D J L 2019 Arctic amplification under global warming of 1.5 and 2 °C in NorESM1-Happi *Earth Syst. Dyn.* **10** 569–98
Hersbach H *et al* 2020 The ERA5 global reanalysis *Q. J. R. Meteorol. Soc.* **146** 1999–2049
Honda M, Inoue J and Yamane S 2009 Influence of low Arctic sea-ice minima on anomalously cold Eurasian winters *Geophys. Res. Lett.* **36** L08707
Jeong J H and Ho C H 2005 Changes in occurrence of cold surges over east Asia in association with Arctic Oscillation *Geophys. Res. Lett.* **32** 1–4
Kaufman Z, Feldl N and Beaulieu C 2024 Warm Arctic–cold Eurasia pattern driven by atmospheric blocking in models and observations *Environ. Res.* **3** 015006
Kim B M, Son S W, Min S K, Jeong J H, Kim S J, Zhang X, Shim T and Yoon J H 2014 Weakening of the stratospheric polar vortex by Arctic sea-ice loss *Nat. Commun.* **5** 4646

King M P, Hell M and Keenlyside N 2016 Investigation of the atmospheric mechanisms related to the autumn sea ice and winter circulation link in the Northern Hemisphere *Clim. Dyn.* **46** 1185–95

Komatsu K K, Takaya Y, Toyoda T and Hasumi H 2022 Response of Eurasian temperature to Barents–Kara Sea ice: evaluation by multi-model seasonal predictions *Geophys. Res. Lett.* **49** 10

Kretschmer M, Adams S V, Arribas A, Prudden R, Saggioro E and Shepherd T G 2021 Quantifying causal pathways of teleconnections *Bull. Am. Meteorol. Soc.* **102** 1–34

Kretschmer M, Coumou D, Agel L, Barlow M, Tziperman E and Cohen J 2018 More-persistent weak stratospheric polar vortex states linked to cold extremes *Bull. Am. Meteorol. Soc.* **99** 49–60

Kretschmer M, Coumou D, Donges J F and Runge J 2016 Using causal effect networks to analyse different Arctic drivers of midlatitude winter circulation *J. Clim.* **29** 4069–81

Kretschmer M, Zappa G and Shepherd T G 2020 The role of Barents—Kara sea ice loss in projected polar vortex changes *Weather Clim. Dyn.* **1** 715–30

L'heureux M 2021 On the sudden stratospheric warming and polar vortex of early 2021 (available at: www.climate.gov/news-features/blogs/enso/sudden-stratospheric-warming-and-polar-vortex-early-2021) (Accessed 13 July 2021)

Liang Y *et al* 2021 Impacts of Arctic sea ice on cold season atmospheric variability and trends estimated from observations and a multimodel large ensemble *J. Clim.* **34** 8419–43

Luo D, Xiao Y, Diao Y, Dai A, Franzke C L E and Simmonds I 2016a Impact of Ural blocking on winter warm Arctic-cold Eurasian anomalies. Part II: the link to the North Atlantic Oscillation *J. Clim.* **29** 3949–71

Luo D, Xiao Y, Yao Y, Dai A, Simmonds I and Franzke C L E 2016b Impact of Ural blocking on winter warm Arctic-cold Eurasian anomalies. Part I: blocking-induced amplification *J. Clim.* **29** 3925–47

McCusker K, Fyfe J and Sigmond M 2016 Twenty-five winters of unexpected Eurasian cooling unlikely due to Arctic sea-ice loss *Nat. Geosci.* **9** 838–42

Mori M, Kosaka Y, Watanabe M, Nakamura H and Kimoto M 2019 A reconciled estimate of the influence of Arctic sea-ice loss on recent Eurasian cooling *Nat. Clim. Change* **9** 123–9

Nakamura T, Yamazaki K, Honda M, Ukita J, Jaiser R, Handorf D and Dethloff K 2016a On the atmospheric response experiment to a Blue Arctic Ocean *Geophys. Res. Lett.* **43** 10,394–402

Nakamura T, Yamazaki K, Iwamoto K, Honda M, Miyoshi Y, Ogawa Y, Tomikawa Y and Ukita J 2016b The stratospheric pathway for Arctic impacts on midlatitude climate *Geophys. Res. Lett.* **43** 3494–501

Nakamura T, Yamazaki K, Iwamoto K, Honda M, Miyoshi Y, Ogawa Y and Ukita J 2015 A negative phase shift of the winter AO/NAO due to the recent Arctic sea-ice reduction in late autumn *J. Geophys. Res.* **120** 3209–27

Nishii K, Taguchi B, Mori M, Kosaka Y and Nakamura H 2022 Arctic sea ice loss and Eurasian cooling in winter 2020−21 *Sci. Online Lett. Atmos.* **18** 199–204

NOAA 2021a Global climate report for January 2021 (available at: www.ncdc.noaa.gov/sotc/global/202101) (Accessed 13 July 2021)

NOAA 2021b Global climate report for February 2021 (available at: www.ncdc.noaa.gov/sotc/global/202102) (Accessed 13 July 2021)

Outten S *et al* 2023 Reconciling conflicting evidence for the cause of the observed early 21st century Eurasian cooling *Weather Clim. Dyn.* **4** 95–114

Peings Y 2019 Ural blocking as a driver of early-winter stratospheric warmings *Geophys. Res. Lett.* **46** 5460–8

Peings Y, Labe Z M and Magnusdottir G 2021 Are 100 ensemble members enough to capture the remote atmospheric response to + 2 °C Arctic sea ice loss? *J. Clim.* **34** 3751–69

Shepherd T G 2021 Bringing physical reasoning into statistical practice in climate-change science *Clim. Change* **169** 2

Siew P Y F, Li C, Sobolowski S P and King M P 2020 Intermittency of Arctic–mid-latitude teleconnections: stratospheric pathway between autumn sea ice and the winter North Atlantic Oscillation *Weather Clim. Dyn.* **1** 261–75

Sun L, Deser C, Simpson I and Sigmond M 2022 Uncertainty in the winter tropospheric response to Arctic Sea ice loss: the role of stratospheric polar vortex internal variability *J. Clim.* **35** 3109–30

Tyrlis E, Manzini E, Bader J, Ukita J, Nakamura H and Matei D 2019 Ural blocking driving extreme Arctic sea ice loss, cold Eurasia, and stratospheric vortex weakening in autumn and early winter 2016–2017 *J. Geophys. Res.* **124** 11313–29

Vargin P N, Koval A V and Guryanov V V 2022 Arctic stratosphere dynamical processes in the winter 2021–2022 *Atmosphere* **13** 1550

Wang S and Chen W 2022 Impact of internal variability on recent opposite trends in wintertime temperature over the Barents–Kara Seas and central Eurasia *Clim. Dyn.* **58** 2941–56

Zappa G, Ceppi P and Shepherd T G 2021 Eurasian cooling in response to Arctic sea-ice loss is not proved by maximum covariance analysis *Nat. Clim. Change* **11** 106–8

Zhang J, Wu Y, Simpson I R, Smith K L, Zhang X, De B and Callaghan P 2018 A stratospheric pathway linking a colder Siberia to Barents-Kara Sea sea ice loss *Sci. Adv.* **4** 1–9